The American Journal of Pathology, Vol. 192, No. 2, February 2022

The American Journal of
PATHOLOGY
ajp.amjpathol.org

GASTROINTESTINAL, HEPATOBILIARY, AND PANCREATIC PATHOLOGY

Experimental Colitis Enhances Temporal Variations in CX3CR1 Cell Colonization of the Gut and Brain Following Irradiation

Ayush Batra,*† Triet M. Bui,* Jacob F. Rehring,* Lenore K. Yalom,* William A. Muller,* David P. Sullivan,* and Ronen Sumagin*

From the Department of Pathology, and the Ken & Ruth Davee Department of Neurology,† Northwestern University Feinberg School of Medicine, Chicago, Illinois*

Accepted for publication October 19, 2021.

Address correspondence to Ronen Sumagin, Ph.D., Department of Pathology, Northwestern University Feinberg School of Medicine, 300 E. Superior St., Chicago, IL 60611. E-mail: ronen.sumagin@northwestern.edu.

Peripheral monocyte-derived CX3C chemokine receptor 1 positive ($CX3CR1^+$) cells play important roles in tissue homeostasis and gut repopulation. Increasing evidence also supports their role in immune repopulation of the brain parenchyma in response to systemic inflammation. Adoptive bone marrow transfer from CX3CR1 fluorescence reporter mice and high-resolution confocal microscopy was used to assess the time course of $CX3CR1^+$ cell repopulation of steady-state and dextran sodium sulfate (DSS)-inflamed small intestine/colon and the brain over 4 weeks after irradiation. $CX3CR1^+$ cell colonization and morphologic polarization into fully ramified cells occurred more rapidly in the small intestine than in the colon. For both organs, the crypt/mucosa was more densely populated than the serosa/muscularis layer, indicating preferential temporal and spatial occupancy. Repopulation of the brain was delayed compared with that of gut tissue, consistent with the immune privilege of this organ. However, DSS-induced colon injury accelerated the repopulation. Expression analyses confirmed increased chemokine levels and macrophage colonization within the small intestine/colon and the brain by DSS-induced injury. Early increases of transmembrane protein 119 and ionized calcium binding adaptor molecule 1 expression within the brain after colon injury suggest immune-priming effect of brain resident microglia in response to systemic inflammation. These findings identify temporal differences in immune repopulation of the gut and brain in response to inflammation and show that gut inflammation can impact immune responses within the brain. *(Am J Pathol 2022, 192: 295–307; https://doi.org/10.1016/j.ajpath.2021.10.013)*

Peripheral monocyte-derived CX3C chemokine receptor 1 positive ($CX3CR1^+$) cells (primarily macrophages and dendritic cells) populate most tissues and organs and represent the highest concentration of mononuclear phagocytes in the body. Over the past several decades, continued evaluation of the function of these innate immune cells marked them as keepers of tissue homeostasis and immune regulation.[1] Particularly in the gut, given constant exposure to commensal microbes, high antigen loads, and high turnover rate of epithelial cells, $CX3CR1^+$ macrophages serve critical roles in dead cell/pathogen clearance, maintenance of immune surveillance, and barrier function.[2] Unlike most other tissue, the constant low-grade inflammatory state of the gut promotes a high turnover rate of $CX3CR1^+$ cells and requires continued replenishment by monocytes circulating in the bloodstream. Interestingly, the structure and function of the gastrointestinal tract dictates compartmentalized localization and function of these cells. For example, within the lamina propria/crypt, villi-associated macrophages are well

Supported by an American Cancer Society Research Scholar Award, Crohn's & Colitis Foundation Senior Research Award, NIH National Institute of Diabetes and Digestive and Kidney Diseases grant R01DK124199 and National Institute of Allergy and Infectious Diseases grant R01AI153568 (R.S.), National Heart, Lung, and Blood Institute grant R35HL155652 (W.A.M.), and the Department of Defense Congressionally Directed Medical Research Programs Horizon Award (T.M.B.).

D.P.S. and R.S. are co-last authors.

Disclosures: None declared.

https://doi.org/10.1016/j.ajpath.2021.10.013

positioned to clear pathogens and food antigens that breach the gut barrier, whereas macrophages in the muscularis externa of the gastrointestinal tract interacting with the enteric nervous system dictate intestinal motility.[3,4]

In the brain, microglial cells under homeostatic conditions self-renew from the original yolk sac lineage throughout the life of the animal.[5] However, under certain pathologic conditions, myeloid precursors, including hematopoietic CX3CR1^{+} macrophages, migrate to the brain parenchyma to contribute to the native microglia population.[6] These engrafted microglia-like cells are able to perform functions similar to native microglial cells with similar morphology, yet maintain a distinct transcriptional and functional identity.[7,8]

Similarly, the brain can recruit perivascular macrophages in disease states. Perivascular macrophages (PVMs) are a distinct self-renewing (in steady state) population of resident brain macrophages that closely associate with and protect the cerebral vasculature and the blood brain barrier. PVMs are not unique to the brain and many other organs use specialized resident macrophage cells to maintain vessel function and local immune surveillance. As such, in the gut, PVMs are fundamental to barrier protection in homeostasis and disease.[9]

The novel connections between the immune response in the gut and brain have been of increasing interest over the past decade. Increased recognition of the pathogenic relevance and crosstalk between the systemic immune response and the brain have sparked further investigation into the links between intestinal inflammation and neuroinflammation.[10] Recent studies have suggested a role for intestinal inflammation in triggering neuroinflammation.[11] Large epidemiologic studies showing strong associations between intestinal inflammation and neurodegenerative disorders such as Alzheimer disease and Parkinson disease further support this hypothesis,[12,13] and have gained significant traction given the increasing prevalence of neurodegenerative diseases across the population. Thus, a deeper understanding of the overlap in immune responses between the gut and the brain is needed and can be achieved by examining common cell types involved and the timing of their recruitment and activation.

Given the increasing significance of the inflammation-mediated overlap between the gut and brain, this study sought to examine the rates of hematopoietic CX3CR1^{+} cell repopulation and morphologic polarization within the gut compartments and the brain. Whole-body gamma irradiation was used to evaluate the temporal course of CX3CR1^{+} cell repopulation in the small intestines/colon and the brain under healthy conditions and in response to intestinal inflammation using a dextran sodium sulfate (DSS) experimental colitis model.

Materials and Methods

Animals

C57BL6J wild-type and CX3CR1-enhanced green fluorescence protein (EGFP) reporter[14] mice were a gift from Dr. Harris Perlman, (Northwestern University, Chicago, IL), and were maintained under specific pathogen-free conditions at the Northwestern University Feinberg School of Medicine animal facilities. At the end of all experimental procedures, animals were euthanized via rapid cervical dislocation. All experimental protocols were approved by the Institutional Animal Care and Use Committee.

Antibodies and Reagents

Nonblocking anti—platelet endothelial cell adhesion molecule 1 antibody (clone 390) for blood vessel labeling was purchased from EMD Millipore (Burlington, MA) and conjugated to DyLight-550 or DyLight-650 using an antibody labeling kit from Thermo Fisher (Waltham, MA) according to the manufacturer's instructions. DSS was purchased from Sigma Aldrich (St. Louis, MO).

Bone Marrow Transfer and Generation of Chimeric Mice

Bone marrow chimeras were generated and maintained using a standard protocol as previously described.[15,16] Ten-week-old wild-type mice were lethally irradiated with a 1000-cGy dose using a Gammacell 40 Exactor ^{137}Cs irradiator (Best Theratronics, Ottawa, ON, Canada) and reconstituted with bone marrow from 8-week-old C57BL/6 CX3CR1-EGFP (heterozygous) reporter mice 24 hours after whole-body irradiation.[17] This method leads to complete replacement of mylomonocytic hematogenic progenitors, as determined using flow cytometry (data not shown). Bone marrow donors and recipients were always matched according to sex. Recipients recovered with trimethoprim and sulfamethoxazole antibiotics in their drinking water to prevent opportunistic infection. Reconstitution was confirmed with flow cytometry and fluorescence imaging of a blood smear (for the presence of EGFP monocytes).

DSS Colitis Model

To induce colon injury and colitis-like symptomatic disease, DSS 3.5% (w/v) was introduced in drinking water for 7 days. Animals subsequently were monitored until specified time points, euthanized, and tissues were processed for further analyses.[18] Disease assessment and animal monitoring was performed as described previously.[19]

Imaging Procedures

Gut Imaging

All imaging of the small intestine and the colon was performed *ex vivo* on freshly excised tissue segments (no fixation or any additional manipulation) immediately after mouse euthanasia. At the specified time points, tissue was excised, laid flat between two glass coverslips, and secured by Vetbond tissue adhesive (3M, St. Paul, MN) to prevent peristaltic movement.

Brain Imaging

All mice underwent a bilateral craniotomy with exposure of the cortical surface to allow for real-time *in vivo* intravital imaging. Mice were anesthetized with ketamine/xylazine 30 minutes before cranial window preparation and placed in a stereotactic frame with a heating pad while undergoing continuous temperature monitoring. The skin and periosteum were removed to expose the skull, and open cranial windows (approximately 5 mm × 5 mm) were generated across each hemisphere using a high-speed dental drill (EXL-M40; Osada, Inc, Los Angeles, CA) lateral to the superior sagittal suture between the bregma and lambda sutures anteriorly and posteriorly, respectively. Heated artificial cerebral spinal fluid buffer solution (Tocris Bioscience, Bristol, UK) was applied directly to the cortical surface just before imaging.

Imaging was performed using an Olympus BX-51WI Fixed-Stage illuminator and equipped with a Yokogawa CSU-X1-A1 spinning disk, a Hamamatsu Electron Multiplying Charge Coupled Device C9100-50 camera, and a Modular Laser System with solid-state diode lasers with diode-pumped solid state modules for 488, 561, and 640 nm and the appropriate filters (all assembled by Perkin Elmer, Naperville, IL) as previously described.[20] Synchronization was managed by a Prosync 2 Synchronization Controller (Piezoystem, Jena, Germany). Z-axis movement and objective positioning was controlled by the Piezoelectric MIPOS100 System (Piezoystem, Jena, Germany). Images were collected using a 20× water-immersion objective (numeric aperture, 1.00). Volocity software (version 6.3; Perkin Elmer, Waltham, MA) was used to drive the microscopy and acquire images, which then were analyzed using ImageJ software version 1.8.0 (NIH, Bethesda, MD; https://imagej.nih.gov/ij).

Image Analysis

To account for cell depth, all images were acquired as Z-stacks of 30 to 40 μm and merged as stack summation for further analyses. All images were analyzed in a blinded fashion by two independent persons (A.B. and J.F.R.). For cell shape and dimension analyses, an ellipsoid was positioned on each individual cell and the longest and shortest axis were recorded for quantification of cell length and width, respectively. Perivascular macrophages were defined as CX3CR1-EGFP$^+$ cells in visible contact with blood vessels.

Gene Expression Analysis

Total RNA from gut and brain tissue was extracted by TRIzol (Applied Biosystems), subjected to DNase I (Promega) treatment (3 U/mL reaction mixture), followed by an additional extraction with TRIzol. An ND-1000 Spectrophotometer (NanoDrop Technologies, Wilmington, DE) was used to assess the quality and concentration of the RNA preparations. RT-PCR was performed with the Applied Biosciences cDNA Synthesis kit (Thermo Scientific, Waltham, MA). Gene expression analyses were performed on total cDNA using the Roche (Basel, Switzerland) SYBR Green Master Kit. The primers for gene-specific analysis by quantitative RT-PCR were custom designed and obtained from IDT (Coralville, IA) or Qiagen (QuantiTect Primer Assays kits, Hilden, Germany). Relative expression analysis was performed using the 2-ΔΔCT method with *GAPDH* serving as the reference gene.

The PCR primers used in the study were all murine-based with the following sequences: CX3CR1 forward: 5′-CAGCATCGACCGGTACCTT-3′; CX3CR1 reverse: 5′-GCTGCACTGTCCGGTTGTT-3′; Cluster of Differentiation 64 (CD64) forward: 5′-TCCTTCTGGAAAATACTGACC-3′, CD64 reverse: 5′-GTTTGCTGTGGTTTGAGACC-3′; C-C chemokine receptor type 2 (CCR2) forward: 5′-ACAGCTCAGGATTAACAGGGACTTG-3′; CCR2 reverse: 5′-ACCACTTGCATGCACACATGAC-3′; ionized calcium binding adaptor molecule 1 (Iba1) forward: 5′-GTCCTTGAAGCGAATGCTGG-3′; Iba1 reverse: 5′-CATTCTCAAGATGGCAGATC-3′; Transmembrane Protein 119 (TMEM119) forward: 5′-GTGTCTAACAGGCCCCAGAA-3′; TMEM119 reverse: 5′-AGCCACGTGGTATCAAGGAG; C-C Motif Chemokine Ligand 2 (CCL2) forward: 5′-CACTCACCTGCTGCTACTCA-3′; CCL2 reverse: 5′-GCTTGGTGACAAAAACTACAGC-3′; CX3CR1 ligand forward: 5′-CGCGTTCTT-CCATTTGTGTA-3′; CX3CR1 ligand reverse: 5′-CTGTGTCGTCTCCAGGACAA-3′; tumor necrosis factor α (TNFα) forward: 5′-CATCTTCTCAAAATTCGAGTGACAA-3′; TNFα reverse: 5′-TGGGAGTAGACAAGGTACAACCC-3′; interleukin 1β forward: 5′-CA-ACCAACAAGTGATATTCTCCATG-3′; interleukin 1β reverse: 5′-GATCCACACTCTCCAGCTGCA-3′; interferon-γ forward: 5′-TCAAGTGGCATAGATGTGGAAGAA-3′; interferon-γ reverse: 5′-TGGCTCTGCAGGA-TTTTCATG-3′; interleukin 17 forward: 5′-ACCTCAA-CCGTTCCACGTCA-3′; interleukin 17 reverse: 5′- CAG-GGTCTTCSTTGCGGTG-3′.

Statistics

Statistical significance was assessed by *t*-test or by one-way analysis of variance with the Newman-Keuls Multiple Comparison Test using GraphPad Prism (V4.0; San Diego, CA) for normally distributed data evaluated using the Shapiro Wilk test. Statistical significance was set at $P < 0.05$. For all experiments the data are shown as ±SEM.

Results

Hematopoietic CX3CR1-EGFP$^+$ Cells Colonize the Small Intestine and the Colon at a Different Rate

Although macrophages in the gut are able to self-sustain, the macrophage pool in the small intestine of adult mice is

maintained primarily through conventional hematopoiesis and is replenished by circulating monocytes. Given the important role macrophages play in intestinal homeostasis and the spatial variations in tissue responses and disease susceptibility between the small and large intestines, we used a bone marrow transplantation (BMT) technique to examine macrophage colonization dynamics of the small intestinal tissue. In these experiments, CX3CR1-EGFP^{+} heterozygous mice (green macrophages) were used as donors and irradiated WT mice as recipients. Appearance, localization, and morphologic changes of grafted CX3CR1-EGFP^{+} macrophages were analyzed over time by confocal microscopy whole-mount imaging of the crypt/mucosa and the serosa/muscularis layers of the small intestine and the colon (as illustrated in Figure 1A). Within 4 weeks of BMT, the number of grafted CX3CR1-EGFP^{+} macrophages had plateaued and that these grafted cells stably populated both the small intestine and the colon. At 4 weeks after BMT, the number of CX3CR1-EGFP^{+} cells in both the crypt/mucosa and the serosa/muscularis layers of the small intestines and the colons of chimeric mice was similar to the number at 10 weeks after BMT and that of control nonchimera CX3CR1-EGFP^{+} reporters, indicating that by week 4 both the small intestine and the colon were fully populated by peripheral CX3CR1-EGFP^{+} cells and that grafted cells fully replaced host cells. Similarly, at 4 weeks after BMT, the number of CX3CR1-EGFP^{+} macrophages in both compartments was not significantly different in chimeric small intestines (Figure 1B) as compared with colon (Figure 1C). However, the crypt/mucosa layers of both organs were populated more densely than the serosa/muscularis layers (61 $\pm$ 16 and 58 $\pm$ 14 versus 32 $\pm$ 7 and 36 $\pm$ 9, respectively) (Figure 1, B and C), indicating preferential spatial occupancy of mononuclear resident cells in the gut. Interestingly, the small intestine was colonized by grafted CX3CR1-EGFP^{+} macrophages more rapidly than the colon in both compartments. The small intestines were fully colonized by week 2 after BMT, whereas the number of CX3CR1-EGFP^{+} macrophages in the colon gradually increased over 4 weeks (Figure 1, B and C). Representative images (Figure 1D)

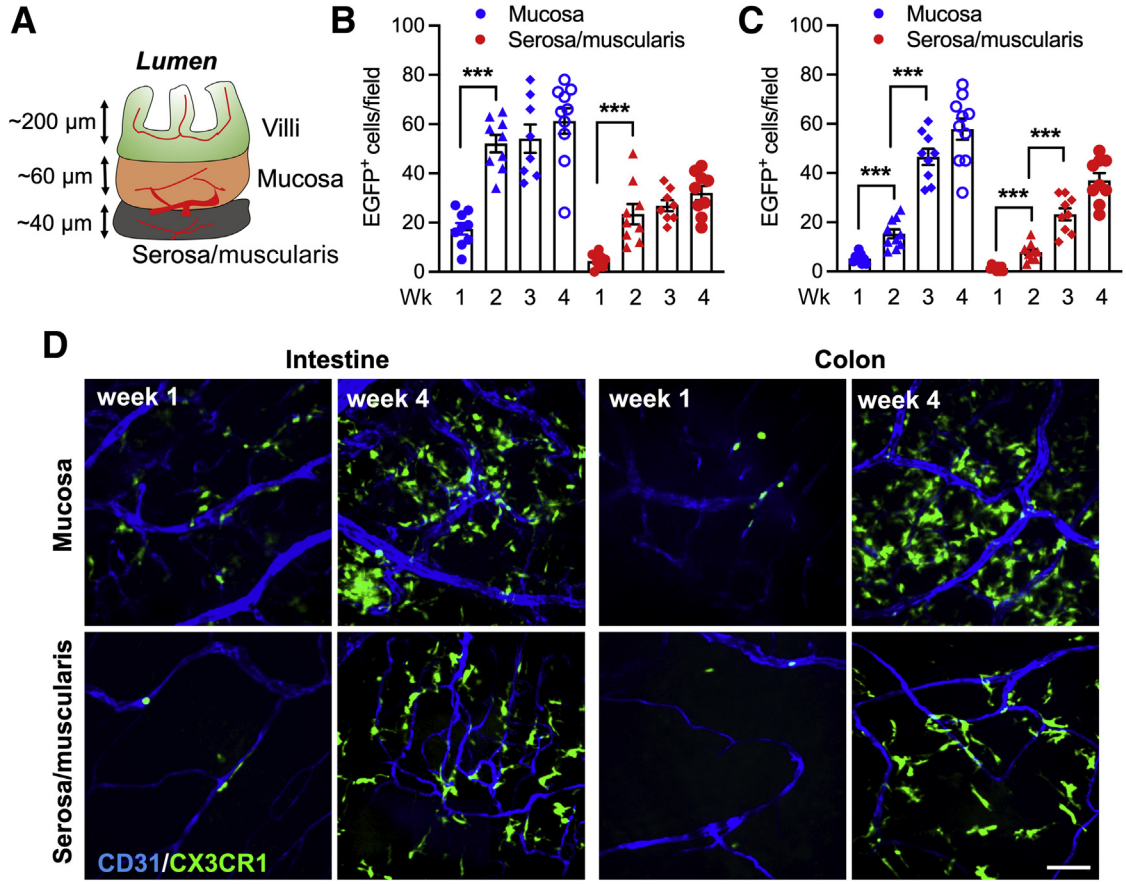

Figure 1 Bone marrow—transferred CX3C chemokine receptor 1—enhanced green fluorescence protein positive (CX3CR1-EGFP^{+}) cells colonize the small intestine and the colon at a different rate. The dynamics of gut colonization by grafted donor CX3CR1-EGFP^{+} BM cells were examined in irradiated wild-type (WT) recipient mice after bone marrow transplantation (BMT). **A:** Depiction of the major tissue compartments in the small intestine. **B** and **C:** Quantification of the number of tissue CX3CR1-EGFP^{+} cells over 4 weeks after BMT in the crypt/mucosa and the serosa/muscularis layers of the intestine and the colon. Grafting of CX3CR1-EGFP^{+} cells in the intestinal compartments was significantly more rapid as compared with the colon. **D:** Representative confocal microscopy images (approximately 20-µm Z-projections) that were in quantitative analyses. Vessels are outlined by CD31 staining (blue). ***$P < 0.001$. Scale bar = 30 µm.

depict CX3CR1-EGFP$^+$ cell colonization of the small intestine and the colon tissue at weeks 1 and 4 after BMT. These data confirm that both the small intestine and the colon can be fully colonized through hematopoiesis and further show the differential dynamics of tissue infiltration by peripheral myeloid cells.

CX3CR1-EGFP$^+$ Cell Morphologic Tissue Polarization Lags in the Colon as Compared with that in the Small Intestine

Monocyte differentiation into tissue macrophages is paralleled by morphologic changes from rounded amoeboid-like cells to fully ramified cells with visible dendrites (illustrated by representative images) (Figure 2A). Therefore, changes in CX3CR1-EGFP$^+$ cell morphology were analyzed during 4 weeks after BMT in the crypt/mucosa and the serosa/muscularis layers of small intestines and the colons. As early as 2 weeks after BMT, more than 60% of CX3CR1-EGFP$^+$ macrophages had progressed to become fully ramified in both the crypt/mucosa and the serosa/muscularis layers of the small intestine. At 3 weeks after BMT, in both compartments, almost all CX3CR1-EGFP$^+$ cells (>90%) completed the morphologic progression (Figure 2, B and C), as seen at steady state in control nonchimeric mice. However, in both compartments of the colon, only approximately 30% of CX3CR1-EGFP$^+$ macrophages were found to be fully ramified at weeks 2 and 3, and approximately 60% at week 4, indicating incomplete/delayed colonization and cell polarization (Figure 2, D and E). These findings show that the small

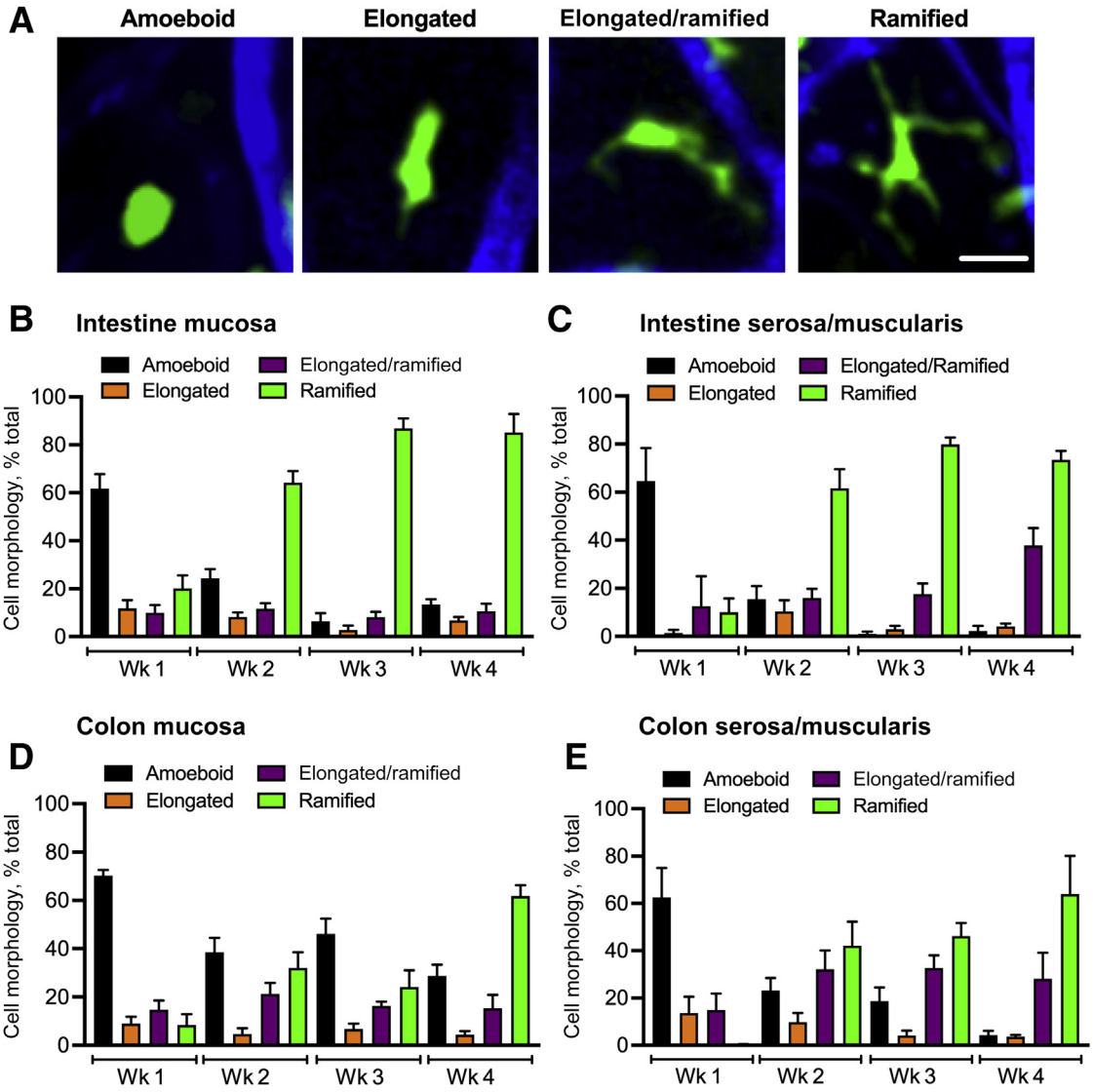

Figure 2 CX3C chemokine receptor 1—enhanced green fluorescence protein positive (CX3CR1-EGFP$^+$) cell morphologic tissue polarization lags in the colon as compared with that in the small intestine. Morphologic polarization of grafted CX3CR1-EGFP$^+$ cells in the crypt/mucosa and the serosa/muscularis layers of the small intestine and the colon was analyzed. **A:** Representative confocal microscopy images depict the sequential changes in the polarization state of grafted CX3CR1-EGFP$^+$ cells. **B**—**D:** Quantitative analyses of the small intestinal (**B** and **C**) and the colon crypt/mucosa and the serosa/muscularis layer (**D** and **E**) depict a gradual shift from mostly ameboid to ramified morphology of grafted cells in the tissue over the 4 weeks after BMT. Scale bar = 20 μm.

intestine is colonized significantly faster by peripheral CX3CR1-EGFP$^+$ cells as compared with the colon and that the small intestine accommodates a more rapid morphologic maturation of these cells. These findings further suggest that peripheral CX3CR1-EGFP$^+$ cells in the tissue require less than a week to undergo full morphologic progression.

Colonic Inflammation/Injury Drives Enhanced Tissue Colonization by CX3CR1-EGFP$^+$ Cells

Whether inflammation and epithelial injury alter the CX3CR1-EGFP$^+$ cell colonization dynamics was investigated next. In these experiments, a cohort of mice was treated with DSS (3.5%, for 7 days in drinking water) immediately after BMT. The changes in numbers and morphology of tissue CX3CR1-EGFP$^+$ cells were analyzed in the small intestinal and colon mucosa at 1 (acute inflammatory) and 3 (resolution phase) weeks after DSS treatment (weeks 2 and 4 after reconstitution after BMT). The treatment regimen is shown in Figure 3A. Control experiments indicated that irradiation and BMT did not significantly impact the DSS treatment outcomes because, with or without irradiation/BMT, peak disease scores ranged between 2.5 and 3, as previously published.[21] Consistent with the relatively minor impact of DSS on the small intestine as compared with that in the colon,[22] no significant difference in the number of colonizing CX3CR1-EGFP$^+$ cells, their morphology, or size, were observed in control versus DSS-treated small intestine (both at weeks 2 and 4 after BMT) (Figure 3, B–D). In contrast, the number of CX3CR1-EGFP$^+$ cells in colon tissue was increased significantly at both time points after DSS treatment (Figure 3E). Despite the increased number of tissue CX3CR1-EGFP$^+$ cells in the colon, the

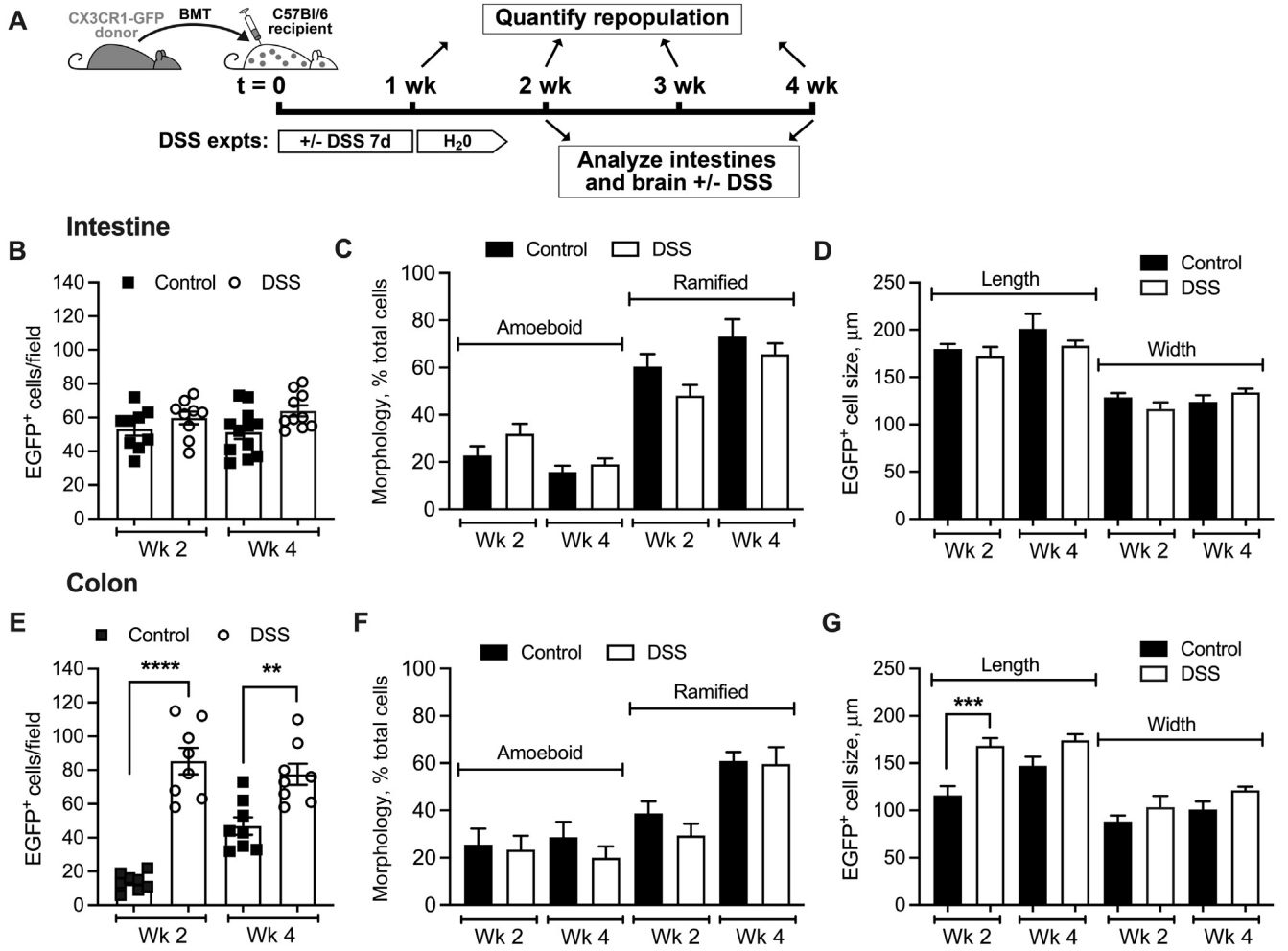

Figure 3 Dextran sodium sulfate (DSS)-induced colon injury promotes tissue engraftment but does not impact CX3C chemokine receptor 1–enhanced green fluorescence protein positive (CX3CR1-EGFP$^+$) cell morphologic polarization. The impact of DSS-induced colon injury on tissue engraftment of CX3CR1-EGFP$^+$ cells after bone marrow transplantation (BMT) was quantified from confocal microscopy imaging. **A:** Schematic outlining the experimental design and the timeline of DSS treatment. **B–G:** Analyses of the number of CX3CR1-EGFP$^+$ cells, morphology, and size in the small intestinal crypt/mucosa (**B–D**) and in the colon crypt/mucosa (**E–G**). Although no significant effects on either of the parameters was noted in the intestine, consistent with the DSS primary impact on the colon, DSS treatment increased the number of tissue CX3CR1-EGFP$^+$ cells and their length without affecting their morphologic polarization. $^{**}P < 0.01$, $^{***}P < 0.001$, and $^{****}P < 0.0001$. DSS, dextran sodium sulfate; expts, experiments; GFP, green fluorescent protein.

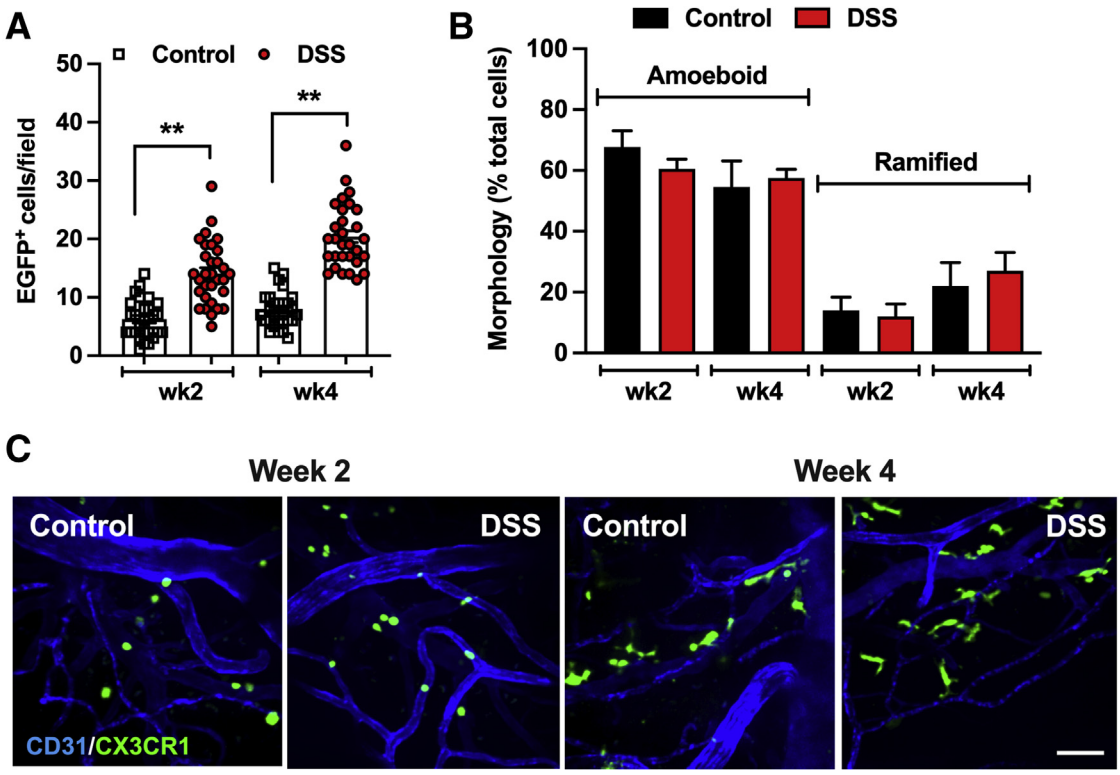

Figure 4 Colon inflammation promotes brain colonization by peripheral CX3C chemokine receptor 1—enhanced green fluorescence protein positive (CX3CR1-EGFP$^+$) cells. CX3CR1-EGFP$^+$ cell infiltration and morphologic polarization were assessed in the brain tissue after bone marrow transplantation (BMT) with/without DSS-induced injury of the colon. **A** and **B:** Quantification of the number of brain tissue CX3CR1-EGFP$^+$ cells (**A**) and CX3CR1-EGFP$^+$ cell morphologic analyses (**B**) at weeks 2 and 4 after BMT. DSS treatment increased the number of engrafted CX3CR1-EGFP$^+$ cells but did not affect their morphologic polarization. **C:** Representative confocal microscopy images (approximately 20-μm Z-projections) that were in quantitative analyses. Vessels are outlined by CD31 staining (blue). $^{**}P < 0.01$. Scale bar = 30 μm. DSS, dextran sodium sulfate.

progression from ameboid to ramified cell morphology was not impacted by tissue inflammation/injury (Figure 3F). Interestingly, in DSS-inflamed colon (week 2), polarized ramified CX3CR1-EGFP$^+$ cells were elongated significantly in size (as measured at the longest axis across the entire cell body), potentially indicating spreading and dendrite extension (Figure 3G). CX3CR1-EGFP$^+$ cell width was increased slightly in the colon, but the change was not significant. In the recovery phase after DSS treatment (week 4), no significant difference between treated and untreated conditions was seen (Figure 3G). These data indicate that although mucosal injury may drive increased recruitment of peripheral cells into the tissue, morphologic polarization of CX3CR1-EGFP$^+$ macrophages is independent of inflammatory cues.

Colon Inflammation Promotes Brain Colonization by Peripheral CX3CR1-EGFP$^+$ Cells

Given the emerging impact of systemic inflammation, particularly gut injury, on brain immune function, whether epithelial injury and gut inflammation impact colonization of the brain by peripheral immune cells was examined next. CX3CR1-EGFP$^+$ macrophage localization and morphologic polarization were assessed in the brain tissue after BMT and whole-body irradiation with/without DSS-induced injury/inflammation of the colon.

Consistent with previous reports,[7] grafted bone marrow—derived CX3CR1-EGFP$^+$ cells successfully populated the brain tissue, despite the well-known immune privilege of this organ. Interestingly, brain colonization by CX3CR1-EGFP$^+$ cells was substantially slower compared with the small intestine or the colon. In steady-state conditions, six ± two and seven ± one CX3CR1-EGFP$^+$ cells per field were found at 2 and 4 weeks after BMT, respectively, which is approximately eight to tenfold lower compared with that in the small intestine and the colon (Figure 4A and representative images in Figure 4B). Importantly, DSS-induced injury/inflammation of the colon substantially increased the number of colonizing CX3CR1-EGFP$^+$ cells in the brain (>twofold) at both time points. These data confirm that systemic/gut inflammation may drive brain repopulation by peripheral immune cells.

Analyses of cell shape further showed that morphologic polarization of grafted CX3CR1-EGFP$^+$ cells was delayed significantly in the brain (compared with small intestinal/colon tissue) and was not impacted by DSS treatment. Although the number of fully ramified CX3CR1-EGFP$^+$

cells in the brain increased over time (from 2 to 4 weeks), it plateaued at approximately 25% of cells (Figure 4B and representative images in Figure 4C). Intriguingly, no significant morphologic differences between gut- and brain-colonizing CX3CR1 cells were noted, indicating that this process is independent of the clearly different microenvironmental cues in these two organs.

Colon Inflammation Promotes Recruitment and Association of CX3CR1-EGFP$^+$ Cells with the Vessel Wall

Because PVMs have emerged as important regulators of vascular function in both the brain and the gut,[9,23] whether peripheral CX3CR1-EGFP$^+$ cells are recruited to the vessel wall after BMT was investigated next. Grafted CX3CR1-

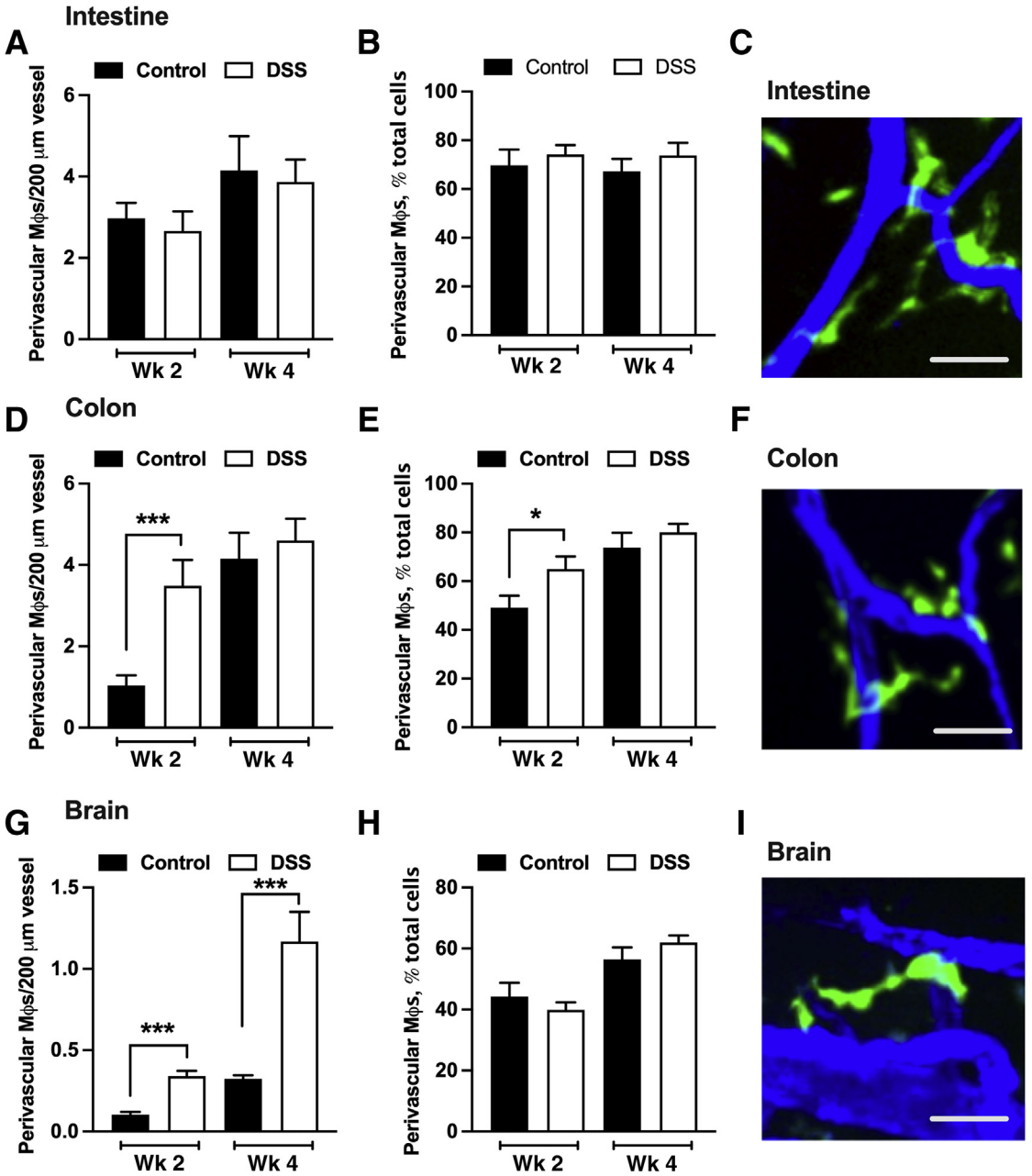

Figure 5 Colon inflammation promotes recruitment of CX3C chemokine receptor 1—enhanced green fluorescence protein positive (CX3CR1-EGFP$^+$) cells to the vessel wall. The number of perivascular CX3CR1-EGFP$^+$ cell (in contact with the vessel) was assessed in gut and brain tissues after bone marrow transplantation (BMT) with/without DSS treatment using confocal microscopy imaging. **A** and **B:** Quantification of the number of perivascular CX3CR1-EGFP$^+$ cells per vessel length and the total number of perivascular CX3CR1-EGFP$^+$ cells per high-power field in the small intestine. **C:** Representative confocal image of perivascular macrophages (green) in the small intestine. **D** and **E:** Perivascular CX3CR1-EGFP$^+$ cell analyses in the colon. **F:** Representative confocal image of colon perivascular CX3CR1-EGFP$^+$ cells. **G**—**I:** Perivascular CX3CR1-EGFP$^+$ cell analyses (**G** and **H**) and representative confocal images of perivascular macrophages (green) in the brain (**I**). DSS treatment increased recruitment and localization of CX3CR1-EGFP$^+$ cells at the vessel wall in the colon and the brain, but not small intestine. **C, F,** and **I:** Blood vessels were stained with CD31 antibody (blue). $^*P < 0.05$, $^{***}P < 0.001$. Scale bars = 25 μm. DSS, dextran sodium sulfate.

EGFP$^+$ cells were indeed recruited to and observed in proximity to blood vessels in steady-state small intestine, the colon, and the brain (Figure 5). In fact, by week 4 after BMT, the majority (>60%) of CX3CR1-EGFP$^+$ cells were found to associate with a blood vessel in all three organs, suggesting physiological significance of these cells in vascular and tissue homeostasis. As expected, given the relatively minor impact of DSS on the small intestine, DSS treatment had no effect on the number of perivascular CX3CR1-EGFP$^+$ cells at the vessel wall or on the fraction of these cells relative to all CX3CR1-EGFP$^+$ cells (Figure 5, A–C). In contrast, in the colon, the number of CX3CR1-EGFP$^+$ cells at the vessel wall was increased significantly by DSS treatment (week 2) and peaked at the resolution phase (week 4) (Figure 5D). Interestingly, at week 2 (colon inflammation/injury), but not week 4 (resolution phase), the fraction of PVMs relative to all CX3CR1-EGFP$^+$ cells also increased significantly, indicating an active recruitment toward the vessel wall (Figure 5, E and F).

Interestingly, DSS-induced colonic inflammation resulted in significant increases in the number of CX3CR1-EGFP$^+$ cells at the vessel wall at 2 weeks, with numbers increasing through 4 weeks after BMT (Figure 5, G and I). These increases in the brain occurred likely owing to increased influx of CX3CR1-EGFP$^+$ cells (Figure 4A), because the relative fraction of CX3CR1-EGFP$^+$ cells at the vessel wall compared with all CX3CR1-EGFP$^+$ cells was not changed (Figure 5H).

Expression Analysis Confirms Increased Macrophage Colonization of the Colon and Brain by DSS-Induced Colon Injury

To complement our imaging analyses, transcriptional analyses by quantitative RT-PCR were performed to examine the expression levels of several key macrophage markers including CX3CR1, CD64, and CCR2 in steady-state (control) and DSS-inflamed colon and the brain. The colon tissue was used because DSS had mild to no effect on the small intestine. Consistent with the DSS-induced increased colon colonization by CX3CR1-EGFP$^+$ cells during the 4 weeks after BMT observed by tissue imaging (Figure 4), significant increases in the expression of CX3CR1 and CD64 (both markers of infiltrating and resident macrophages) as well as CCR2 (which more selectively marks monocyte-derived infiltrating cells) were observed both at the acute inflammatory (week 2) and the resolution (week 4) phases (Figure 6A). This was true for brain expression analyses, in which transcript levels of CX3CR1 and CCR2 were increased up to 80-fold by DSS treatment (Figure 6B). Iba1 has been used previously to mark brain-infiltrating macrophages, whereas TMEM119 is a selective marker for brain resident microglia cells.[24] Expression analyses of these markers showed significant increases in the acute phase after DSS (week 2), but the expression of both proteins was reduced substantially during the resolution phase (week 4) (Figure 6C), indicating potential polarization of infiltrating cells toward the resident phenotype. These data confirm that injury to the colon drives cellular changes and immune cell colonization of the brain.

DSS-Induced Inflammation in the Colon Increases Macrophage Chemotactic Ligands in the Brain

Finally, to more mechanistically address the impact of DSS treatment on CX3CR1-EGFP$^+$ cell colonization of the colon and the brain, expression levels of relevant receptor ligands/chemokines were examined within tissues in acute and resolution phases (weeks 2 and 4, respectively). Consistent with the DSS treatment–induced epithelial erosion/decreased crypt density and increased immune infiltrate (representative histology images) (Figure 7A), expression of several key inflammatory cytokines was found to be increased significantly in the acute phase in the colon (week 2) (Figure 7B). Cytokine levels were decreased significantly in the resolution phase (week 4). Importantly, increased levels of CX3CR1 ligand and CCL2 were observed both at weeks 2 and 4 (Figure 7C), consistent with the CX3CR1-EGFP$^+$ cell colonization of the colon mucosa.

In the brain, where peripheral CX3CR1-EGFP$^+$ cell infiltration is delayed substantially as compared with that in the colon, and the number of colonizing cells continually increased over the 4 weeks after BMT, increases in tissue CX3CR1 ligand and CCL2 were more pronounced at week 4 after BMT (Figure 7E). Interestingly, although chemokine levels were increased in brain tissue and peripheral CX3CR1-EGFP$^+$ cell infiltration was increased after DSS treatment, no histologic features of brain inflammation, including tissue fibrosis, hypoxia, or lymphocytic infiltrate, were observed (representative histology images) (Figure 7D). Similarly, although a significant induction in TNFα levels indicating potential priming was detected in the brain, no significant changes in other inflammatory markers were observed (Figure 7F).

Discussion

Given the high turnover of immune cells in the gut, it is imperative to better understand their repopulation dynamics and patterns in healthy and diseased tissue. Furthermore, given recent evidence of gut inflammation impacting the function and immune responses in the brain, exploring molecular and mechanistic links in this process is essential. Thus, in the current work, BM transfer of fluorescent reporter immune cells and advanced tissue imaging was used to temporally and spatially characterize repopulation and morphologic patterns during steady state and in inflamed gut and brain. Significant differences in the way both the small intestines and colon are repopulated by innate immune cells

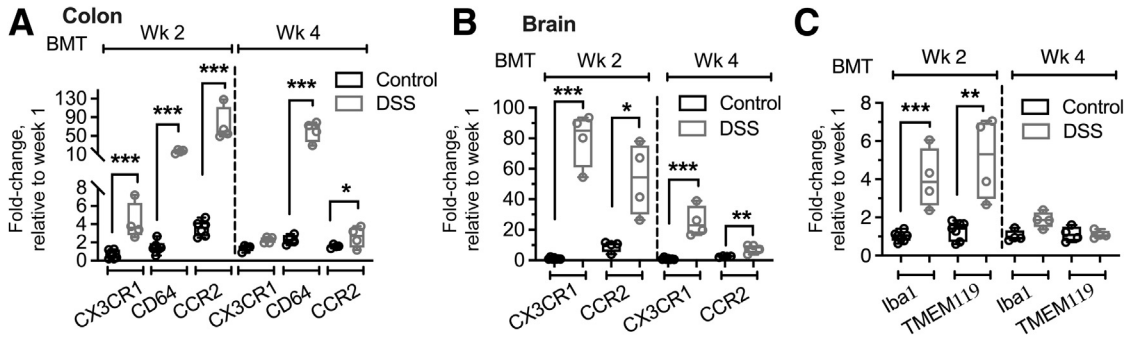

Figure 6 Expression analyses confirm increased macrophage colonization of the colon and the brain by dextran sodium sulfate (DSS)-induced colon injury. Transcription analyses by quantitative RT-PCR for common macrophage markers were performed in steady-state (control) and DSS-inflamed colon and the brain. **A** and **B:** Quantitative analyses of CX3C chemokine receptor 1 (CX3CR1), CD64, and C-C chemokine receptor type 2 (CCR2) in the colon (**A**) and the brain (**B**) showed significant increases in transcript levels after DSS treatment, consistent with an increased number of engrafting CX3CR1-enhanced green fluorescence protein positive $(EGFP)^+$ cells in both colon and brain tissue. **C:** Transcription analyses of more selective brain macrophage and microglia markers ionized calcium binding adaptor molecule 1 (Iba1) and transmembrane protein 119 (TMEM119) showed similar increases after DSS treatment in the acute (week 2) but not resolution (week 4) phase. $*P < 0.05$, $**P < 0.01$, and $***P < 0.001$. BMT, bone marrow transplantation; Wk, week.

were identified and a significant impact of gut inflammation on brain immunity was confirmed.

Without apparent inflammation, the small intestine was repopulated by circulating immune cells at a significantly increased rate compared with the colon. Epithelial protein turnover is significantly slower in the colon than in the small intestine.[25] This indicates a slower rate of tissue turnover in the colon, which is consistent with the current observations in immune cells. Epithelial turnover is impacted by the host microbiome, which is perhaps not surprising because the small intestine and the colon have distinct microbial habitats. Indeed, turnover of intestinal and colonic macrophages is influenced significantly by the local microbiota, and artificial depletion of resident microbiota or exposure to antibiotics impairs the turnover of these macrophages.[9] Furthermore, despite the increased length of the small intestine, the transit time in the small intestine compared with the colon is an order of magnitude shorter than that of the colon,[26] undoubtedly contributing to the more rapid cellular turnover. The mucus layer is another factor that may contribute to both epithelial and especially immune cell turnover in the gut. Although the small intestine harbors a single, tightly attached mucus layer, mucus on the colon is organized into two distinct layers, with the inner mucus layer being practically sterile (assessed by fluorescence *in situ* hybridization[27]). As such, exposure of the lamina propria—residing immune cells to commensal or opportunistic microbes is increased significantly in the small intestine as compared with the colon, likely driving increased turnover rates. Consistently, DSS-induced experimental colitis, which leads to epithelial injury and increases cell turnover, significantly boosted immune repopulation in the colon without impacting the small intestine.

Interestingly, the small intestinal/colon mucosa was populated more densely by CX3CR1 cells than the muscularis layer, indicating preferential spatial occupancy of mononuclear resident cells in the gut. This is consistent with observations from single-cell RNA sequencing of immune cells in various intestinal compartments, suggesting that resident macrophages throughout the gut are functionally distinct and perform niche-specific roles based on localization.[4]

Macrophage cell shape can reflect resident versus inflammatory polarization states as has been shown previously *in vitro*.[28] Changes in CX3CR1-$EGFP^+$ cell morphology were evaluated because these cells entered steady-state or inflamed tissues. As expected, most CX3CR1-$EGFP^+$ cells in tissues progressed from ameboid to ramified cell morphology in both the gut and the brain. Surprisingly, their morphologic polarization was largely not impacted by DSS treatment. The exception was the acute inflammatory state in the colon (week two after DSS), in which CX3CR1-$EGFP^+$ cells were significantly more elongated, potentially indicating spreading and dendrite extension. This is consistent with the barrier breach resulting from DSS-induced colon injury. Although it appears that *in vivo* morphologic polarization of CX3CR1-$EGFP^+$ macrophages is independent of inflammatory cues, whether cell shape represents the polarization state remains to be determined.

Unlike the gut, the brain is largely populated by yolk sac—derived macrophages during embryogenesis, which specialize to serve its unique immune surveillance needs.[29] This includes specialized patrolling microglia within the brain and perivascular spaces that provide structural and functional support for healthy and diseased brain tissue. After whole-body irradiation, the brain was infiltrated by peripheral CX3CR1-$EGFP^+$ cells and that more than approximately 50% of CX3CR1-$EGFP^+$ cells entering the brain localized to blood vessels (consistent with the critical role PVMs play in maintenance of the blood-brain barrier). The repopulation of the brain was enhanced significantly by DSS-induced inflammation and injury to the colon. The partial loss of resident microglia resulting from irradiation likely contributed to CX3CR1-$EGFP^+$ cell entry into the brain, whereas tight junction disruption and the presence of inflammatory cytokines after DSS treatment, as has been

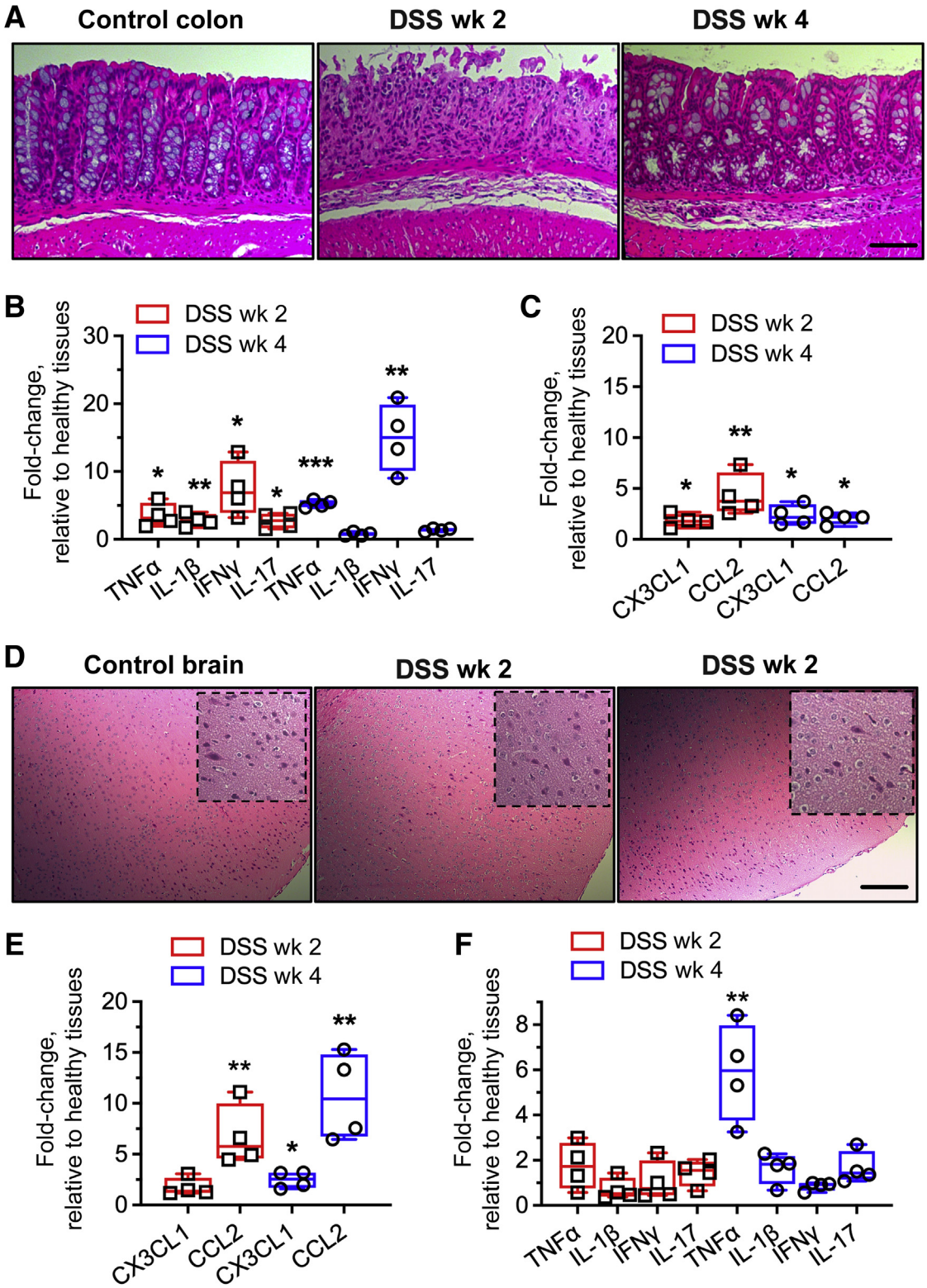

Figure 7 Dextran sodium sulfate (DSS)-induced inflammation in the colon increases macrophage chemotactic ligands in the brain. **A:** Representative histology images of healthy and DSS-treated colon (treatment was for 1 week) in the acute and resolution phases (weeks 2 and 4 after BMT, respectively). **B** and **C:** Transcription analyses for inflammatory cytokine panel (**B**) and major macrophage chemokines (**C**) were performed in steady-state (control) and DSS-treated colon. **D:** Representative brain cortex histology images with/without DSS treatment. **Dotted lines** define higher-magnification zoom-in images. **E** and **F:** Transcription analyses for major macrophage chemokines (**E**) and inflammatory cytokines (**F**) in brain tissue at weeks 2 and 4 after BMT and DSS treatment. As expected, increases in chemokine and cytokine expression were found in the colon, confirming DSS-induced inflammation. Chemokine expression was increased similarly over time in the brain, however, only increases in TNFα were detected. $^{*}P < 0.05$, $^{**}P < 0.01$, and $^{***}P < 0.001$. Scale bars = 100 μm. CCL2, C-C chemokine receptor type 2; IFN, interferon; IL, interleukin.

shown previously, likely induced further increases in CX3CR1-EGFP$^+$ cell colonization of the brain parenchyma.[30,31] Although in agreement with previous work,[30] increased levels of TNFα were observed in the brain, but gross morphologic inflammatory features were not detected in brains of DSS-treated mice (Figure 7D). Lower rates of CX3CR1-EGFP$^+$ cell repopulation were observed within the brain compared with the gut with and without DSS treatment. This is possibly a result of the immune privilege of the brain, relative resistance of resident microglia to irradiation, and their increased longevity compared with the resident immune cells of the gut.[31–33]

Expression analyses showed increased levels of TMEM119 during the acute inflammatory phase, highlighting activation of innate immunity of the central nervous system after an induction of colonic inflammation. TMEM119 is a cell-specific marker of embryologic resident central nervous system microglia,[34] which serve an essential function of translating peripheral immune signals to the brain to alter function.[35] In response to inflammatory stimuli, resident microglia become activated, featuring increased expression of TMEM119 and a morphologic shift from a ramified (resting state) to an ameboid (activated state) shape. Although morphologic differences in brain-infiltrating CX3CR1-EGFP$^+$ cells were not detected, increased TNFα and cortical CCL2 levels were observed in response to DSS-induced colitis. This indicates that signaling from the colon during colitis may prime resident macrophage-like cells in remote organs, such as the brain, for potential pathogenic insult. The absence of any significant lymphocytic infiltrate and other histologic features of inflammation in the brain parenchyma supports the idea of immune priming by colon injury, but not an induction of full-scale neuroinflammation. Previous work has shown that the primary neurologic insult in conjunction with the systemic inflammatory insult (such as in the case of sepsis or even colitis) can worsen neurologic outcomes. For example, mouse models of traumatic brain injury and cortical microinfarcts show exacerbation of neurologic injury in the setting of acute colitis.[36,37] The underlying mechanisms for this exacerbated injury to the brain are not yet well defined but are likely to involve the compromise of blood-brain barrier integrity. Although the cerebral vasculature is responsible for the regulated trafficking of proteins and cells within the brain parenchyma, PVMs localize to these vessels and play important roles in maintaining vascular function in the brain. As such, future studies that aim to evaluate specific endothelial-derived chemokines that mediate PVM recruitment and how PVMs regulate barrier integrity will be critical to better understand the mechanisms of neurologic injury secondary to systemic immune responses. In summary, the current findings identify novel patterns of innate immune cell colonization of the gut and the brain and confirm the link between inflammation in the gut and immune responses in the brain. An impact of gut inflammation on neurologic outcomes in health and disease have dramatic clinical implications. Further research into the mechanisms of gut inflammation priming immune capabilities in the brain is needed to understand this translationally relevant pathophysiology.

Acknowledgments

We thank Dr. Harris Perlman, Ph.D. (Northwestern University) for the CX3CR1-EGFP reporter mice and the Pathology Core Facility of the Robert H. Lurie Comprehensive Cancer Center, Northwestern University, for help with tissue slides and hematoxylin and eosin staining.

References

1. Mowat AM, Agace WW: Regional specialization within the intestinal immune system. Nat Rev Immunol 2014, 14:667–685
2. Takiishi T, Fenero CIM, Camara NOS: Intestinal barrier and gut microbiota: shaping our immune responses throughout life. Tissue Barriers 2017, 5:e1373208
3. De Schepper S, Stakenborg N, Matteoli G, Verheijden S, Boeckxstaens GE: Muscularis macrophages: key players in intestinal homeostasis and disease. Cell Immunol 2018, 330:142–150
4. Viola MF, Boeckxstaens G: Niche-specific functional heterogeneity of intestinal resident macrophages. Gut 2021, 70:1383–1395
5. Ajami B, Bennett JL, Krieger C, Tetzlaff W, Rossi FM: Local self-renewal can sustain CNS microglia maintenance and function throughout adult life. Nat Neurosci 2007, 10:1538–1543
6. Davoust N, Vuaillat C, Androdias G, Nataf S: From bone marrow to microglia: barriers and avenues. Trends Immunol 2008, 29:227–234
7. Cronk JC, Filiano AJ, Louveau A, Marin I, Marsh R, Ji E, Goldman DH, Smirnov I, Geraci N, Acton S, Overall CC, Kipnis J: Peripherally derived macrophages can engraft the brain independent of irradiation and maintain an identity distinct from microglia. J Exp Med 2018, 215:1627–1647
8. Shemer A, Grozovski J, Tay TL, Tao J, Volaski A, Suss P, Ardura-Fabregat A, Gross-Vered M, Kim JS, David E, Chappell-Maor L, Thielecke L, Glass CK, Cornils K, Prinz M, Jung S: Engrafted parenchymal brain macrophages differ from microglia in transcriptome, chromatin landscape and response to challenge. Nat Commun 2018, 9:5206
9. Honda M, Surewaard BGJ, Watanabe M, Hedrick CC, Lee WY, Brown K, McCoy KD, Kubes P: Perivascular localization of macrophages in the intestinal mucosa is regulated by Nr4a1 and the microbiome. Nat Commun 2020, 11:1329
10. Doney E, Cadoret A, Dion-Albert L, Lebel M, Menard C: Inflammation-driven brain and gut barrier dysfunction in stress and mood disorders. Eur J Neurosci 2021, [Epub ahead of print] doi: https://doi.org/10.1111/ejn.15239
11. Chen QQ, Haikal C, Li W, Li JY: Gut inflammation in association with pathogenesis of Parkinson's disease. Front Mol Neurosci 2019, 12:218
12. Singh A, Dawson TM, Kulkarni S: Neurodegenerative disorders and gut-brain interactions. J Clin Invest 2021, 131:e143775
13. Houser MC, Tansey MG: The gut-brain axis: is intestinal inflammation a silent driver of Parkinson's disease pathogenesis? NPJ Parkinsons Dis 2017, 3:3
14. Zheng Z, Chiu S, Akbarpour M, Sun H, Reyfman PA, Anekalla KR, Abdala-Valencia H, Edgren D, Li W, Kreisel D, Korobova FV, Fernandez R, McQuattie-Pimentel A, Zhang ZJ, Perlman H, Misharin AV, Scott Budinger GR, Bharat A: Donor pulmonary

intravascular nonclassical monocytes recruit recipient neutrophils and mediate primary lung allograft dysfunction. Sci Transl Med 2017, 9: eaal4508
15. Sullivan DP, Dalal PJ, Jaulin F, Sacks DB, Kreitzer G, Muller WA: Endothelial IQGAP1 regulates leukocyte transmigration by directing the LBRC to the site of diapedesis. J Exp Med 2019, 216: 2582−2601
16. Duran-Struuck R, Dysko RC: Principles of bone marrow transplantation (BMT): providing optimal veterinary and husbandry care to irradiated mice in BMT studies. J Am Assoc Lab Anim Sci 2009, 48:11−22
17. Jung S, Aliberti J, Graemmel P, Sunshine MJ, Kreutzberg GW, Sher A, Littman DR: Analysis of fractalkine receptor CX(3)CR1 function by targeted deletion and green fluorescent protein reporter gene insertion. Mol Cell Biol 2000, 20:4106−4114
18. Whittem CG, Williams AD, Williams CS: Murine colitis modeling using dextran sulfate sodium (DSS). J Vis Exp 2010, 35:1652
19. Butin-Israeli V, Bui TM, Wiesolek HL, Mascarenhas L, Lee JJ, Mehl LC, Knutson KR, Adam SA, Goldman RD, Beyder A, Wiesmuller L, Hanauer SB, Sumagin R: Neutrophil-induced genomic instability impedes resolution of inflammation and wound healing. J Clin Invest 2019, 129:712−726
20. Sullivan DP, Bui T, Muller WA, Butin-Israeli V, Sumagin R: In vivo imaging reveals unique neutrophil transendothelial migration patterns in inflamed intestines. Mucosal Immunol 2018, 11:1571−1581
21. Bui TM, Butin-Israeli V, Wiesolek HL, Zhou M, Rehring JF, Wiesmuller L, Wu JD, Yang GY, Hanauer SB, Sebag JA, Sumagin R: Neutrophils alter DNA repair landscape to impact survival and shape distinct therapeutic phenotypes of colorectal cancer. Gastroenterology 2021, 161:225−238.e15
22. Chassaing B, Aitken JD, Malleshappa M, Vijay-Kumar M: Dextran sulfate sodium (DSS)-induced colitis in mice. Curr Protoc Immunol 2014, 104:15.25.1−15.25.14
23. Goldmann T, Wieghofer P, Jordao MJ, Prutek F, Hagemeyer N, Frenzel K, Amann L, Staszewski O, Kierdorf K, Krueger M, Locatelli G, Hochgerner H, Zeiser R, Epelman S, Geissmann F, Priller J, Rossi FM, Bechmann I, Kerschensteiner M, Linnarsson S, Jung S, Prinz M: Origin, fate and dynamics of macrophages at central nervous system interfaces. Nat Immunol 2016, 17:797−805
24. Gonzalez Ibanez F, Picard K, Bordeleau M, Sharma K, Bisht K, Tremblay ME: Immunofluorescence staining using IBA1 and TMEM119 for microglial density, morphology and peripheral myeloid cell infiltration analysis in mouse brain. J Vis Exp 2019, 152
25. Arike L, Seiman A, van der Post S, Rodriguez Pineiro AM, Ermund A, Schutte A, Backhed F, Johansson MEV, Hansson GC: Protein turnover in epithelial cells and mucus along the gastrointestinal tract is coordinated by the spatial location and microbiota. Cell Rep 2020, 30:1077−1087.e3
26. Donaldson GP, Lee SM, Mazmanian SK: Gut biogeography of the bacterial microbiota. Nat Rev Microbiol 2016, 14:20−32
27. Hansson GC, Johansson ME: The inner of the two Muc2 mucin-dependent mucus layers in colon is devoid of bacteria. Gut Microbes 2010, 1:51−54
28. McWhorter FY, Wang T, Nguyen P, Chung T, Liu WF: Modulation of macrophage phenotype by cell shape. Proc Natl Acad Sci U S A 2013, 110:17253−17258
29. Wu Y, Hirschi KK: Tissue-resident macrophage development and function. Front Cell Dev Biol 2020, 8:617879
30. Han Y, Zhao T, Cheng X, Zhao M, Gong SH, Zhao YQ, Wu HT, Fan M, Zhu LL: Cortical inflammation is increased in a DSS-induced colitis mouse model. Neurosci Bull 2018, 34:1058−1066
31. Morganti JM, Jopson TD, Liu S, Gupta N, Rosi S: Cranial irradiation alters the brain's microenvironment and permits CCR2+ macrophage infiltration. PLoS One 2014, 9:e93650
32. Willis EF, MacDonald KPA, Nguyen QH, Garrido AL, Gillespie ER, Harley SBR, Bartlett PF, Schroder WA, Yates AG, Anthony DC, Rose-John S, Ruitenberg MJ, Vukovic J: Repopulating microglia promote brain repair in an IL-6-dependent manner. Cell 2020, 180: 833−846.e16
33. Shaw TN, Houston SA, Wemyss K, Bridgeman HM, Barbera TA, Zangerle-Murray T, Strangward P, Ridley AJL, Wang P, Tamoutounour S, Allen JE, Konkel JE, Grainger JR: Tissue-resident macrophages in the intestine are long lived and defined by Tim-4 and CD4 expression. J Exp Med 2018, 215:1507−1518
34. Bennett ML, Bennett FC, Liddelow SA, Ajami B, Zamanian JL, Fernhoff NB, Mulinyawe SB, Bohlen CJ, Adil A, Tucker A, Weissman IL, Chang EF, Li G, Grant GA, Hayden Gephart MG, Barres BA: New tools for studying microglia in the mouse and human CNS. Proc Natl Acad Sci U S A 2016, 113:E1738−E1746
35. Hoogland IC, Houbolt C, van Westerloo DJ, van Gool WA, van de Beek D: Systemic inflammation and microglial activation: systematic review of animal experiments. J Neuroinflammation 2015, 12:114
36. Hanscom M, Loane DJ, Aubretch T, Leser J, Molesworth K, Hedgekar N, Ritzel RM, Abulwerdi G, Shea-Donohue T, Faden AI: Acute colitis during chronic experimental traumatic brain injury in mice induces dysautonomia and persistent extraintestinal, systemic, and CNS inflammation with exacerbated neurological deficits. J Neuroinflammation 2021, 18:24
37. Chen X, He X, Luo S, Feng Y, Liang F, Shi T, Huang R, Pei Z, Li Z: Vagus nerve stimulation attenuates cerebral microinfarct and colitis-induced cerebral microinfarct aggravation in mice. Front Neurol 2018, 9:798